

Modelling an electrolyser in a graph-based framework

Buu-Van Nguyen^{a,*}, Johan Romate^b and Cornelis Vuik^c

^a*Delft Institute of Applied Mathematics, Technische Universiteit Delft, Delft, The Netherlands*

^b*Technische Universiteit Delft, Delft, The Netherlands*

^c*Delft Institute of Applied Mathematics, Technische Universiteit Delft, Delft, The Netherlands*

ARTICLE INFO

Keywords:

Electrolyser
Integrated energy network
Multi-carrier energy systems
Steady-state load flow analysis
Well-posedness

ABSTRACT

We propose an electrolyser model for steady-state load flow analysis of multi-carrier energy networks, where the electrolyser is capable of producing hydrogen gas and heat. We show that there are boundary conditions that lead to a well-posed problem. We derive these conditions for two cases, namely with a fixed and non-fixed ratio between gas and heat output. Furthermore, the derived conditions are validated numerically.

1. Introduction

The current level of greenhouse gas emissions leads to a significant contribution towards global warming [10][9]. A straightforward solution to global warming is to reduce the level of emissions. This can be achieved by replacing fossil fuels partly with renewable energy sources, such as solar and wind energy [1][6]. The downside of these sources is that it can lead to an unstable power system [8][2][18][15]. The instability is caused by the variable energy production, due to the dependence on the weather. Fortunately, it is possible to prevent instability of the energy system by using electrolysers. An electrolyser can convert a surplus of electricity into hydrogen gas and heat. While an insufficient amount of energy is produced, the hydrogen gas produced by electrolysers can be utilised to offset the deficiency. However, utilising an electrolyser efficiently, requires a careful analysis on the placement and quantity of electrolysers in the energy network. The analysis is usually done by modelling the energy transport, also known as a load flow analysis. The difficulty in modelling the effect of an electrolyser accurately, is that you have to model multiple energy carriers. In our case, those are electricity, gas and heat, which results in an integrated energy network.

A way to model multi-carrier energy networks is by using a graph-based framework [13] [11] [12]. The graph-based framework allows modelling a variety of coupling units, but an electrolyser has not been well researched in this framework. The closest coupling unit is a Power-to-Gas (P2G) unit and an electrical boiler, but it only captures conversion to 1 energy carrier, whilst an electrolyser outputs to different energy carriers. A combined heat and power plant (CHP) is another coupling unit that outputs to different energy carriers. Although, the input energy is different from an electrolyser, which is gas.

In this paper, we show a linear model for an electrolyser that can be utilised for steady-state load flow analysis. We show that boundary conditions exist that lead to a well-posed

problem. Moreover, we include some numerical experiments to illustrate our approach.

2. Model

We model an electrolyser that can convert electricity into gas and residual heat, where we are interested in two cases. The first case considers an electrolyser where it converts gas and heat with a known output ratio. The second case considers a situation where the output ratio has to be determined depending on the energy transport surrounding the electrolyser.

Before we start with the model equations, we need a graph representation of an electrolyser. Therefore, we describe how an energy network can be transformed into a graph. A graph consists of nodes connected by links. Each node and link corresponds to an energy network element. For example, a node can represent a source and a link can represent a transmission line. Moreover, each node and link corresponds to a physical law. Explicitly, the nodes are associated with conservation laws and the links are associated with the physical model of the underlying network element. Table 1 shows an overview of the conservation laws and common models for each single-carrier. The models for each single-carrier represents the following: the electrical network is an AC system [17][11], the gas network is a low-pressure system [14][11] and the heat network is a closed-loop system [11].

Since an electrolyser interacts with different energy-carriers, it is modelled as a node connected with links of the relevant energy carriers. We assume that these links have no energy losses. The coupling node, that represents an electrolyser, has a model that governs the energy balance given by Equation (1):

$$\eta P = \text{HHV}q + \Delta\varphi \quad (1)$$

where $\eta \in [0, 1]$ is the efficiency, P is the active power, q is the gas flow, HHV is the higher heating value of gas and $\Delta\varphi$ is the heat power. This model is based on the CHP model from [16] [19], where we have adjusted our model based on the input and output energy. However, a CHP can generate electricity and heat in a flexible manner, whilst for

*Corresponding author

✉ b.nguyen@tudelft.nl (B. Nguyen)

Table 1
Models for electricity, gas and heat networks.

	Network element	Description	Model
Electricity	Node	Kirchhoff's law for active power	$P_i = -\sum_j P_{ij}$
	Node	Kirchhoff's law for reactive power	$Q_i = -\sum_j Q_{ij}$
	Link	Short transmission line (send, P)	$P_{ij} = g_{ij} V_i ^2 - V_i V_j (g_{ij} \cos \delta_{ij} + b_{ij} \sin \delta_{ij})$
	Link	Transmission line (send, Q)	$Q_{ij} = -b_{ij} V_i ^2 - V_i V_j (g_{ij} \sin \delta_{ij} - b_{ij} \cos \delta_{ij})$
	Link	Transmission line (receive, P)	$P_{ji} = g_{ij} V_j ^2 - V_i V_j (g_{ij} \cos \delta_{ij} - b_{ij} \sin \delta_{ij})$
	Link	Transmission line (receive, Q)	$P_{ji} = -b_{ij} V_j ^2 + V_i V_j (g_{ij} \sin \delta_{ij} + b_{ij} \cos \delta_{ij})$
Gas	Node	Conservation of mass	$q_i = \sum_j q_{ij}$
	Link	Pipe	$p_i - p_j = (C^g)^{-2} f q_{ij} q_{ij}$
Heat	Node	Conservation of mass	$m_i = \sum_j m_{ij}$
	Node	Conservation of energy (supply)	$\sum_l m_{i,l} T_{i,l}^s = \sum_j m_{ij} T_{ij}^s$
	Node	Conservation of energy (return)	$\sum_l m_{i,l} T_{i,l}^r = \sum_j m_{ij} T_{ij}^r$
	Link	Pipe	$p_i - p_j = (C^h)^{-2} f m_{ij} m_{ij}$
	Link	Pipe heat loss (supply)	$T_{ji}^s = T^a + e^{\frac{hxDL}{c_p m}} (T_{ij}^s - T^a)$
	Link	Pipe heat loss (return)	$T_{ij}^r = T^a + e^{\frac{hxDL}{c_p m}} (T_{ji}^r - T^a)$
	Terminal link	Total heat power	$\Delta\varphi_{i,l} = C_p m_{i,l} (T_{i,l}^s - T_{i,l}^r)$

an electrolyser only residual heat is available. This behaviour is reflected by Equation (2):

$$\eta_h \eta P = \Delta\varphi \quad (2)$$

where $\eta_h \in [0, 1]$ is the heat efficiency. In other words, Equation (2) tells us that a fraction of the available energy is converted to heat. Henceforth, we require two equations to model an electrolyser that converts electricity into gas and heat.

Our model allows the electrolyser to produce gas and heat in a flexible manner by letting η_h to be unknown. Hence, our model is capable of modelling both cases we mentioned in the beginning of this section. From a mathematical point of view, we seek to know when the model is well-posed for these cases. Therefore, we show necessary conditions for when this holds in Section 3.

3. Boundary conditions

In general, integrated energy networks lead to a system of nonlinear equations. These systems are usually solved numerically. Solving a nonlinear energy system is conventionally done with the Newton-Raphson (NR) method. In this method a linearisation of the system of equations is involved, where one has to solve a linear system in order to solve the original system. With regards to linear systems, a necessary condition for well-posedness is that the system of equations is square. Usually, energy network models have more variables than equations, unless we allow additional conditions in the form of specifying variables. In this paper, we denote them as boundary conditions. A side note, nodes with different types of boundary conditions are known as node types in literature related to electrical networks.

To understand which conditions need to be met for a well-posed system including an electrolyser, we start with a simple network. We investigate an electrolyser with one node

of each single-carrier attached to it. The graph network of this is shown in Figure 1.

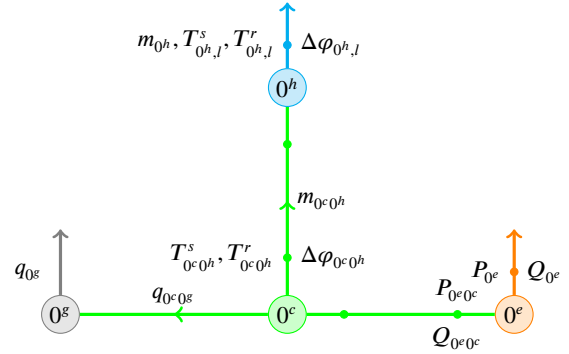


Figure 1: A graph representation of an electrolyser. Node 0^c and the connecting dummy links represent the electrolyser. Node 0^g is a node of the gas network. Node 0^h is a node of the heat network. Node 0^e is a node of the electrical network. For each node, except node 0^c , a terminal link is connected to it. This link represents energy flowing in or out of the network.

Well-posedness conditions must hold for elementary cases, such as an electrolyser only generating one of the energy outputs, gas or heat. This reduces down to a P2G unit or an electrical boiler. Leading to an analysis of two networks, which are shown in Figure 2 and Figure 3.

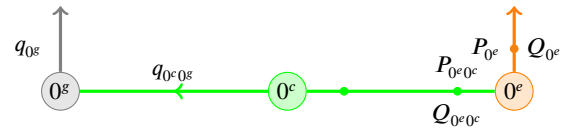


Figure 2: A coupling between an electrical and a gas network with an electrolyser. This is equivalent to modelling a P2G unit.

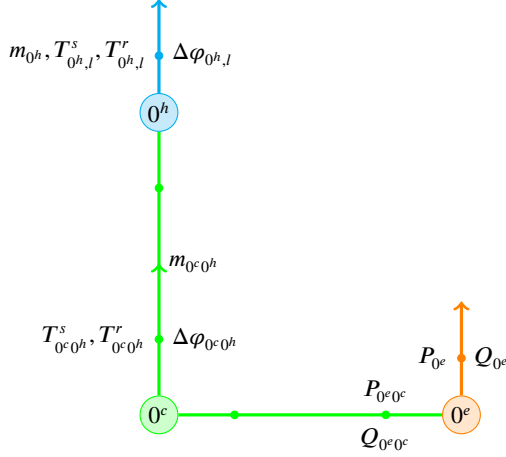


Figure 3: A coupling between an electrical and a heat network with an electrolyser. This is equivalent to modelling an electrical boiler

Based on our initial model, we can model a P2G unit or an electrical boiler by setting the heat efficiency to 0 or 1. Alternatively, the mass flow $m_{0^c0^h}$ or the gas flow $q_{0^e0^g}$ is set to 0.

In the remainder of this section, we derive boundary conditions for 2 cases, a known heat efficiency and unknown heat efficiency.

3.1. Known heat efficiency

In this section, we assume that the heat efficiency η_h of the electrolyser is given. Furthermore, we are interested in the production of gas and heat based on a given active power. It is also possible to specify the gas flow or heat power instead of the active power, which gives us a similar analysis. Henceforth, we focus on one case, which is the case with a specified active power. We start with deriving the boundary conditions for the P2G unit, then the electrical boiler. Finally, we combine the boundary conditions leading to well-posedness conditions for the electrolyser.

P2G

A P2G unit has the following model [3] [5]:

$$\eta P = \text{HHV}q \quad (3)$$

where $\eta \in [0, 1]$. One can obtain an equivalent model with the electrolyser model (1)-(2) by assuming that $\eta_h = 0$. The system of equations corresponding to the network shown in Figure 2 is represented as:

$$P_{0^e} + P_{0^e0^c} = 0 \quad (4)$$

$$Q_{0^e} + Q_{0^e0^c} = 0 \quad (5)$$

$$q_{0^e0^g} - q_{0^g} = 0 \quad (6)$$

$$\eta P_{0^e0^c} - \text{HHV}q_{0^c0^g} = 0 \quad (7)$$

We require a square system for well-posedness. HHV is a known parameter, so we have 4 equations and 6 unknown variables. To obtain a square system we must specify 2

variables.

We assume that the input energy, P_{0^e} , is known. We let $Q_{0^e,0^c} = 0$. This choice is motivated from a physical point of view. Note that we have an AC model for the electrical network. The electrolyser model (3) does not depend on the reactive power, because we assume that an electrolyser requires a DC input [18]. We also assume that there are no energy losses from converting AC to DC. Hence, the reactive power can be any arbitrary constant, we have chosen 0 for convenience. With these assumptions, we now have a square system and the boundary conditions are presented in Table 2.

Table 2

Known heat efficiency: boundary conditions for a P2G unit.

Node	Known	Unknown
0^g		q_{0^g}
0^e	P_{0^e}	Q_{0^e}
0^c	$Q_{0^e0^c} = 0$	$q_{0^c0^g}, P_{0^c0^e}$

Note that the system is linear. With our boundary conditions, the matrix resulting from this system is non-singular. Therefore, a unique solution exists. Thus our boundary conditions lead to a well-posed problem.

Electrical Boiler

An electrical boiler is modelled with [20]:

$$\Delta\varphi_{0^c0^h} = \eta P_{0^e0^c} \quad (8)$$

This model is equivalent to the electrolyser model (1)-(2) whenever $\eta_h = 1$, because this results in $q_{0^c0^h} = 0$. We consider the model described in Equation (8) for the sake of brevity. The network shown in Figure 3 results in the following system of equations:

$$P_{0^e} + P_{0^e0^c} = 0 \quad (9)$$

$$Q_{0^e} + Q_{0^e0^c} = 0 \quad (10)$$

$$m_{0^c0^h} - m_{0^h} = 0 \quad (11)$$

$$m_{0^c0^h} T_{0^c0^h}^s - m_{0^h} T_{0^h,l}^s = 0 \quad (12)$$

$$-m_{0^c0^h} T_{0^c0^h}^r + m_{0^h} T_{0^h,l}^r = 0 \quad (13)$$

$$C_p m_{0^h} (T_{0^h,l}^s - T_{0^h,l}^r) - \Delta\varphi_{0^h,l} = 0 \quad (14)$$

$$\eta P_{0^e0^c} - \Delta\varphi_{0^c0^h} = 0 \quad (15)$$

$$C_p m_{0^c0^h} (T_{0^c0^h}^s - T_{0^c0^h}^r) - \Delta\varphi_{0^c0^h} = 0 \quad (16)$$

Equation (16) is a new addition compared to the P2G case. This equation is required, because it describes how the heat consumption is related to the mass flow and temperature for a heat sink and source.

We assume that the specified heat constant C_p is known. It follows that our system has 8 equations and 12 unknowns. To obtain a square system, we have to specify 4 variables. We let the electrolyser generate heat with a specified active power P_{0^e} . Resulting in node 0^e to be a load node. From equations (14) and (16), it follows that a reference temperature is required for a unique solution. Thus, we assume that the

return temperature $T_{0^h,l}^r$ is specified. The third variable to be specified is the supply temperature of the electrical boiler $T_{0^e0^c}^s$, because we assume that the provided heat comes out at a set temperature. The last variable we specify is the reactive power, $Q_{0^e0^c} = 0$, we do this for the same reason as for the P2G unit. The assumptions are summarised in Table 3.

Table 3

Known heat efficiency: boundary conditions for an electrical boiler.

Node	Known	Unknown
0^h	$T_{0^h,l}^r$	$m_{0^h}, T_{0^h,l}^s, \Delta\varphi_{0^h,l}$
0^e	P_{0^e}	Q_{0^e}
0^c	$Q_{0^e0^c} = 0, T_{0^e0^c}^s$	$m_{0^c0^h}, T_{0^c0^h}^r, \Delta\varphi_{0^c0^h}, P_{0^c0^e}$

These boundary conditions lead to a unique solution. The derivation is shown below.

1. The reactive power Q_{0^e} is obtained from Equation (10):

$$Q_{0^e} = -Q_{0^e0^c}$$

2. From Equation (9) we obtain the active power P_{0^e} :

$$P_{0^e} = -P_{0^e0^c}$$

3. Equation (15) yields the heat power $\Delta\varphi_{0^c0^h}$:

$$\Delta\varphi_{0^c0^h} = \eta P_{0^e0^c}$$

4. The supply temperature $T_{0^h,l}^s$ is obtained from Equation (12):

$$T_{0^h,l}^s = \frac{m_{0^c0^h}}{m_{0^h}} T_{0^c0^h}^s \stackrel{(11)}{=} T_{0^c0^h}^s$$

5. From Equation (13), we express the return temperature $T_{0^c0^h}^r$ as:

$$T_{0^c0^h}^r = \frac{m_{0^h}}{m_{0^c0^h}} T_{0^h,l}^r \stackrel{(11)}{=} T_{0^h,l}^r$$

6. Applying the results provided in steps 4 and 5 on equations (14) and (16) yields the total heat power $\Delta\varphi_{0^c0^h}$:

$$\Delta\varphi_{0^c0^h} = \Delta\varphi_{0^h,l}$$

7. The mass flow $m_{0^c0^h}$ is obtained from Equation (16):

$$m_{0^c0^h} = \frac{\Delta\varphi_{0^c0^h}}{C_p(T_{0^c0^h}^s - T_{0^c0^h}^r)}$$

8. The mass flow m_{0^h} is derived from Equation (11):

$$m_{0^h} = m_{0^c0^h}$$

Thus all variables can be determined uniquely. Henceforth, we can conclude that the conditions shown in Table 3 lead to a well-posed problem.

Electrolyser

We have derived boundary conditions for the P2G unit and electrical boiler, which can be seen as special cases of the electrolyser with one output energy. Now we consider the electrolyser with both its output capabilities. The system of equations is given below:

$$P_{0^e} + P_{0^e0^c} = 0 \quad (17)$$

$$Q_{0^e} + Q_{0^e0^c} = 0 \quad (18)$$

$$q_{0^c0^g} - q_{0^g} = 0 \quad (19)$$

$$m_{0^c0^h} - m_{0^h} = 0 \quad (20)$$

$$m_{0^c0^h} T_{0^c0^h}^s - m_{0^h} T_{0^h,l}^s = 0 \quad (21)$$

$$-m_{0^c0^h} T_{0^c0^h}^r + m_{0^h} T_{0^h,l}^r = 0 \quad (22)$$

$$C_p m_{0^h} (T_{0^h,l}^s - T_{0^h,l}^r) - \Delta\varphi_{0^h,l} = 0 \quad (23)$$

$$C_p m_{0^c0^h} (T_{0^c0^h}^s - T_{0^c0^h}^r) - \Delta\varphi_{0^c0^h} = 0 \quad (24)$$

$$\eta P_{0^e0^c} - \text{HHV} q_{0^c0^g} - \Delta\varphi_{0^c0^h} = 0 \quad (25)$$

$$\eta_h \eta P_{0^e0^c} - \Delta\varphi_{0^c0^h} = 0 \quad (26)$$

Recall that η_h is known. This leads to a system with 10 equations and 14 unknowns. Therefore, we have to specify 4 variables. We combine the boundary conditions derived for the P2G unit and electrical boiler to obtain boundary conditions for the electrolyser. This results in the conditions shown in Table 4.

Table 4

Known heat efficiency: boundary conditions for an electrolyser.

Node	Known	Unknown
0^e	P_{0^e}	Q_{0^e}
0^g		q_{0^g}
0^h	$T_{0^h,l}^r$	$m_{0^h}, T_{0^h,l}^s, \Delta\varphi_{0^h,l}$
0^c	$Q_{0^e0^c} = 0, T_{0^e0^c}^s$	$q_{0^c0^g}, P_{0^c0^e}, m_{0^c0^h}, T_{0^c0^h}^r, \Delta\varphi_{0^c0^h}$

A unique solution can be obtained in a similar fashion as for the electrical boiler. We conclude that the boundary conditions lead to a well-posed problem.

3.2. Unknown heat efficiency

Our model allows the electrolyser to output gas and heat with any arbitrary ratio, which is equivalent to an unknown heat efficiency η_h . Compared to the case with a known heat efficiency, we have to specify an additional variable. Otherwise there are an infinite amount of choices for the output ratio of gas and heat. We model a case where both output energies are known, so that we have to compute the required input energy for the electrolyser. This leads to the active power to be unknown and the gas flow and heat power to be known. We note that other cases with 2 specified energy streams can be chosen, but those lead to a similar analysis. We have the same set of equations as in the case with a known heat efficiency. With an unknown heat efficiency, the system has 10 equations and 15 unknowns, so 5 variables have to be specified. Since we want the output energies

to be known, we let node 0^g to be a load node and node 0^h to be a sink. Hence, we specify q_{0^g} and $\Delta\varphi_{0^h,l}$. The reactive power $Q_{0^e0^e}$, the coupling supply temperature $T_{0^e0^h}^s$ and the return temperature $T_{0^h,l}^r$ are known. These variables follow the same reasoning as for the case with a known heat efficiency. The boundary conditions are shown in table 5.

Table 5

Unknown heat efficiency: boundary conditions for an electrolyser.

Node	Known	Unknown
0^g	q_{0^g}	
0^h	$\Delta\varphi_{0^h,l} > 0, T_{0^h,l}^r$	$m_{0^h}, T_{0^h,l}^s$
0^e	P_{0^e}, Q_{0^e}	
0^c	$Q_{0^e0^e} = 0, T_{0^e0^h}^s$	$q_{0^e0^g}, P_{0^e0^e}, m_{0^e0^h}, T_{0^e0^h}^r, \Delta\varphi_{0^e0^h}$

Applying these boundary conditions for our system of equations and solving it in a similar fashion as we have seen in section 3.1 for the electrical boiler, we obtain a unique solution. Thus the boundary conditions results in a well-posed problem.

3.3. Electrolyser coupled with single-carrier systems

In the previous sections, we have investigated a network with one electrolyser without any physical links connected to it, so energy losses from the connected single-carrier networks are not modelled. To show the effect of an electrolyser in a more realistic energy network setting, we simply extend the network shown in Figure 1 with one physical link for each single-carrier network. The extended link of the gas and heat network represents a pipe. The link for the electrical network represents a transmission line. The network is shown in Figure 4.

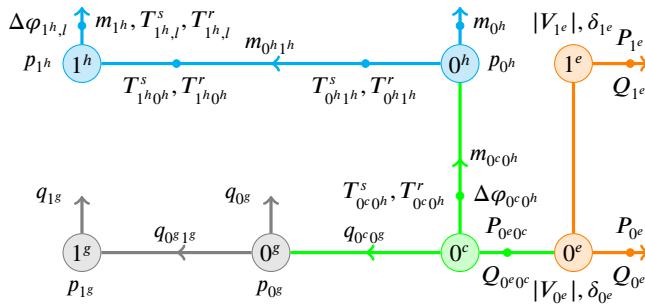


Figure 4: The network shown in Figure 1 is extended with physical links for each energy carrier. Node 0^e , 0^g and 0^h are acting as junctions. Whilst node 1^e , 1^g and 1^h are sources or sinks.

Nodes 0^e , 0^g and 0^h are junctions. The junctions are modelled in a conventional way by assuming that no energy can enter or escape the network. This forces our load nodes from our previous network (0^e , 0^g and 0^h) to move to node 1^e , 1^g and 1^h in the current network. The resulting system of equations is shown in Appendix C, which has 18 equations

and 30 unknown variables whenever the heat efficiency is known.

For these systems, the same well-posedness conditions derived in Section 3.1 with a known heat efficiency and Section 3.2 with an unknown heat efficiency are applied for loads 1^e , 1^g and 1^h . The gas and heat network require reference pressures. The reference pressure can be placed on a junction or a load node in their respective network. We have chosen to place them on the loads. Also the coupling node 0^c has the same boundary conditions that we have derived before. The resulting boundary conditions that lead to well-posedness for a known and unknown heat efficiency are shown in Table 6 and 7.

Table 6

Known heat efficiency: boundary conditions for an electrolyser with physical links.

Node	Known	Unknown
0^e	$P_{0^e} = 0, Q_{0^e} = 0$	V_{0^e}, δ_{0^e}
1^e	$P_{1^e}, V_{1^e}, \delta_{1^e}$	Q_{1^e}
0^g	$q_{0^g} = 0$	p_{0^g}
1^g	p_{1^g}	q_{1^g}
0^h	$m_{0^h} = 0$	p_{0^h}
1^h	$p_{1^h}, T_{1^h,l}^r$	$p_{1^h}, T_{1^h,l}^s, \Delta\varphi_{1^h,l}$
0^c	$Q_{0^e0^e} = 0, T_{0^e0^h}^s$	$q_{0^e0^g}, P_{0^e0^e}, m_{0^e0^h}, T_{0^e0^h}^r, \Delta\varphi_{0^e0^h}$

Table 7

Unknown heat efficiency: boundary conditions for an electrolyser with physical links.

Node	Known	Unknown
0^e	$P_{0^e} = 0, Q_{0^e} = 0$	V_{0^e}, δ_{0^e}
1^e	V_{1^e}, δ_{1^e}	P_{1^e}, Q_{1^e}
0^g	$q_{0^g} = 0$	p_{0^g}
1^g	$q_{1^g} > 0, p_{1^g}$	
0^h	$m_{0^h} = 0$	p_{0^h}
1^h	$p_{1^h}, \Delta\varphi_{1^h,l} > 0, T_{1^h,l}^r$	$m_{1^h}, T_{1^h,l}^s$
0^c	$Q_{0^e0^e} = 0, T_{0^e0^h}^s$	$q_{0^e0^g}, P_{0^e0^e}, m_{0^e0^h}, T_{0^e0^h}^r, \Delta\varphi_{0^e0^h}$

An analytical solution is not easy to derive, due to the nonlinear equations in our system. Therefore, we validate our results numerically.

4. Numerical Results

In this section, we numerically solve the system representing an electrolyser with physical links shown in Figure 4. We do this with a known and unknown heat efficiency. Recall that there are some assumptions that hold for this energy network. Firstly, the electrical network is modelled as an AC system. Secondly, we assume a low-pressure system for the gas network. Lastly, the heat network is modelled as a closed-loop system with a supply and return line. Moreover, specification of the transmission lines, gas and pipes are summarised in Appendix B. Additionally, the efficiencies of the electrolyser are found in the same section.

We solve the system with the Newton-Raphson (NR) method,

where the stopping criterion is defined as:

$$\|F\|_2 \leq 10^{-6}$$

For the inner solve we have used an LU factorisation from the SuperLU package [4].

The system of equations has 18 equations and variables. By substitution, we are able to reduce the system to 15 equations and variables. The initial guess for the NR method is given in Table 8. We motivate our choices as follows. The mass flows are chosen such that they are nonzero, otherwise the Jacobian is singular. The supply and return temperatures are determined such that the average of these temperatures equals the temperature of the boundary condition for the supply temperature T_{0e0h}^s . The pressure in the gas network p_{0g} is chosen such that the pressure drop is nonzero, because a pressure drop of zero leads to a singular Jacobian. Likewise for the pressure p_{0h} in the heat network. The voltage magnitude $|V_{0e}|$ is based on a flat start with same value as the boundary condition. The other variables are set to 0 out of convenience.

Table 8

Known heat efficiency: the initial guess.

Electricity		Gas		
$ V_{0e} $	δ_{0e}	p_{0g}	q_{0g1g}	
$\frac{690}{\sqrt{3}}\text{V}$	0rad	1.05bar	$0\frac{\text{kg}}{\text{s}}$	
Heat				
T_{0h1h}^s	T_{1h0h}^r	p_{0h}	T_{1h1h}^s	m_{0h1h}
353.15K	313.15K	6.3bar	353.15K	$1\frac{\text{kg}}{\text{s}}$
Coupling				
P_{0e0e}	q_{0e0h}	m_{0e0h}	T_{0e0h}^r	$\Delta\varphi_{0e0h}$
0MW	$0\frac{\text{kg}}{\text{s}}$	$1\frac{\text{kg}}{\text{s}}$	313.15K	0MW

With this initial guess, the NR method converges in 5 iterations. The numerical solution is shown in Table 9.

We observe reasonable energy losses caused by the physical links. In the electrical network, the transmission line shows a loss in active power. In absolute value it drops by 0.066MW. For the gas network, we observe a small pressure drop of $\Delta p = 0.003\text{bar}$. Similarly, for the heat network, a pressure drop of $\Delta p = 0.048\text{bar}$ is noted. For the supply temperature from node 0^h to 1^h , the temperature drops by 0.27K. The return temperature in the direction from node 1^h to 0^h drops by 0.208K. Thus our model behaves as expected. For the case with an unknown heat efficiency, we have chosen boundary condition values, such that we have the same numerical solution as for the known heat efficiency case. Moreover, we have observed similar convergence behaviour with the NR method.

The results for the electrolyser with physical links suggest that the problem is well-posed.

Table 9

Known heat efficiency: solution of an electrolyser with physical links. The values of the boundary conditions are in bold.

Electricity				
$ V_{0e} $	δ_{0e}	P_{0e}	Q_{0e}	$ V_{1e} $
375V	-0.259rad	0MW	0MW	398V
δ_{1e}	P_{1e}	Q_{1e}	P_{0e1e}	Q_{0e1e}
0rad	-2.5MW	-0.662MW	-2.434MW	0MW
P_{1e0e}	Q_{1e0e}			
2.5MW	0.662MW			
Gas				
p_{0g}	q_{0g}	P_{1g}	q_{1g}	q_{0g1g}
1.003bar	$0\frac{\text{kg}}{\text{s}}$	1bar	$0.013\frac{\text{kg}}{\text{s}}$	$0.013\frac{\text{kg}}{\text{s}}$
Heat				
p_{0h}	m_{0h}	$T_{0h1h}^s(T_{0h}^s)$	P_{1h}	m_{1h}
6.048bar	$0\frac{\text{kg}}{\text{s}}$	338.15K	6bar	$5.74\frac{\text{kg}}{\text{s}}$
$T_{1h1h}^s(T_{1h}^s)$	T_{1h1h}^r	$T_{1h0h}^r(T_{1h}^r)$	$\Delta\varphi_{1h}$	m_{0h1h}
337.88K	323.15K	323.15K	0.354MW	$5.74\frac{\text{kg}}{\text{s}}$
Coupling				
P_{0e0e}	Q_{0e0e}	q_{0e0h}	m_{0e0h}	$\Delta\varphi_{0e0h}$
2.434MW	0MW	$0.013\frac{\text{kg}}{\text{s}}$	$5.74\frac{\text{kg}}{\text{s}}$	0.365MW
T_{0e0h}^s	$T_{0e0h}^r(T_{0h}^r)$			
338.15K	322.942K			

5. Conclusion

We have introduced a linear model for the electrolyser. This model is used within a steady-state load flow analysis of multi-carrier energy networks. Furthermore, we have focused on energy networks that consist of 3 different energy carriers. These energy carriers are electricity, gas and heat. In this context, we are interested when the inclusion of the electrolyser model lead to a well-posed problem. We have validated our results analytically as well as numerically. The results of the electrolyser connected with physical links suggest that the links can be replaced with networks, since the boundary conditions connected with the electrolyser are the determining factor for well-posedness. In other words, if these boundary conditions are chosen such that they coincide with a known or unknown heat efficiency case, then well-posedness is expected for a broader set of network topologies. Therefore, our electrolyser model can be used in a larger setting than just one physical link per energy carrier.

A. Nomenclature

Electricity	
δ	Voltage angle [rad]
P	Active power [W]
Q	Reactive power [var]
V	Voltage phasor [V]
$ V $	Voltage amplitude [V]
Gas	
f	Friction factor
q	Gas flow rate [$\text{kg} \cdot \text{s}^{-1}$]
C_g	Pipe constant [$\text{kg}^2 \cdot \text{m}^2$]
Heat	
φ	Heat power [W]
$\Delta\varphi$	Total heat power [W]
T	Temperature [K]
m	Mass flow rate [$\text{kg} \cdot \text{s}^{-1}$]
C_h	Pipe constant [$\text{kg} \cdot \text{m}$]
C_p	Specific heat [$\text{m}^2 \cdot \text{K}^{-1} \cdot \text{s}^{-2}$]
General	
p	Pressure [Pa]

B. System specification

Table 10

Physical properties of the electrical system.

	Variable	Value
	Power system	AC
Line	B (Susceptance)	-0.3 S
	G (Conductance)	0.03 S

Table 11

Physical properties of the gas system.

	Variable	Value
	Pressure system	Low pressure
	Gas type	Hydrogen gas
	HHV	$1.418 \cdot 10^8 \frac{\text{J}}{\text{kg}}$
	S (Specific gravity)	0.589
	Z (Compressibility factor)	1
	p_n (Standard pressure)	1 bar
	T_n (Standard temperature)	288 K
	R (Ideal gas constant)	$8.314413 \frac{\text{J}}{\text{molK}}$
	M (Molar mass of air)	$28.97 \cdot 10^{-3} \frac{\text{kg}}{\text{mol}}$
Pipe	L	500 m
	D	0.15 m
	f (Friction factor)	$6.5 \cdot 10^{-3}$

Table 12

Physical properties of the heat system.

	Variable	Value
	ρ (density of water)	$960 \frac{\text{kg}}{\text{m}^3}$
	C_p (Specific heat of water)	$4.182 \cdot 10^3 \frac{\text{J}}{\text{kgK}}$
	g (gravitational constant)	$9.81 \frac{\text{kg}}{\text{s}^2}$
	T_a (ambient temperature)	273.15 K
Pipe	L	500 m
	D	0.15 m
	λ (Heat transfer coefficient)	$0.2 \frac{\text{W}}{\text{m}^2 \cdot \text{K}}$
	f (Friction factor)	$6.5 \cdot 10^{-3}$

Table 13

Electrolyser efficiency.

Variable	Value
η	$\frac{9}{10}$
η_h	$\frac{7}{6}$

C. System of equations of an electrolyser with physical links

The system of equations is shown below:

$$P_{0e} + P_{0e1e} + P_{0e0c} = 0 \quad (27)$$

$$Q_{0e} + Q_{0e1e} + Q_{0e0c} = 0 \quad (28)$$

$$P_{1e} + P_{1e0e} = 0 \quad (29)$$

$$Q_{1e} + Q_{1e0e} = 0 \quad (30)$$

$$q_{0c0g} - q_{0g1g} - q_{0g} = 0 \quad (31)$$

$$q_{0g1g} - q_{1g} = 0 \quad (32)$$

$$p_{0g} - p_{1g} - (C^g)^{-2} f^g |q_{0g1g}| q_{0g1g} = 0 \quad (33)$$

$$m_{0h1h} - m_{1h} = 0 \quad (34)$$

$$m_{0c0h} - m_{0h1h} - m_{0h} = 0 \quad (35)$$

$$p_{0h} - p_{1h} - (C^h)^{-2} f^h |m_{0h1h}| m_{0h1h} = 0 \quad (36)$$

$$m_{0c0h} T_{0c0h}^s - m_{0h1h} T_{0h1h}^s = 0 \quad (37)$$

$$-m_{0c0h} T_{0c0h}^r + m_{0h1h} T_{0h1h}^r = 0 \quad (38)$$

$$m_{0h1h} T_{1h0h}^s - m_{1h} T_{1h,l}^s = 0 \quad (39)$$

$$-m_{0h1h} T_{1h0h}^r + m_{1h} T_{1h,l}^r = 0 \quad (40)$$

$$C_p m_{1h} (T_{1h,l}^s - T_{1h,l}^r) - \Delta\varphi_{1h,l} = 0 \quad (41)$$

$$C_p m_{0c0h} (T_{0c0h}^s - T_{0c0h}^r) - \Delta\varphi_{0c0h} = 0 \quad (42)$$

$$\eta P_{0e0c} - \text{HHV} q_{0c0g} - \Delta\varphi_{0c0h} = 0 \quad (43)$$

$$\eta_h \eta P_{0e0c} - \Delta\varphi_{0c0h} = 0 \quad (44)$$

Let $\delta_{ij} = \delta_i - \delta_j$. We use 0 and 1 as a shorthand notation for node 0^e and 1^e . We define the active and reactive power on the transmission line as:

$$P_{10} = g_{10} |V_1|^2 - |V_0| |V_1| (g_{10} \cos \delta_{10} + b_{10} \sin \delta_{10})$$

$$P_{01} = g_{01} |V_0|^2 - |V_0| |V_1| (g_{01} \cos \delta_{01} - b_{01} \sin \delta_{01})$$

$$Q_{10} = -b_{10} |V_1|^2 - |V_0| |V_1| (g_{10} \sin \delta_{10} - b_{10} \cos \delta_{10})$$

$$Q_{01} = -b_{01}|V_0|^2 + |V_0||V_1| (g_{01} \sin \delta_{01} + b_{01} \cos \delta_{01})$$

These are substituted in equations (29)-(30). Hence, the active and reactive power corresponding to the transmission line are no longer present in the system of equations. Instead the voltage magnitude and voltage angle are introduced into the system of equations.

For the heat network, assuming that $m_{0h1h} > 0$, the temperature at the end of a supply line and return line are substituted in the relevant equations by:

$$T_{1h0h}^s = (T_{0h1h}^s - T^a) e^{\frac{-\lambda}{C_p m_{0h1h}} L} + T^a$$

$$T_{0h1h}^r = (T_{1h0h}^r - T^a) e^{\frac{-\lambda}{C_p m_{0h1h}} L} + T^a$$

This leads to a system of 18 equations and 30 unknown variables whenever η_h is known.

CRedit authorship contribution statement

Buu-Van Nguyen: Conceptualization, Methodology, Software, Writing - Original Draft. **Johan Romate:** Writing - review & editing, Supervision. **Cornelis Vuik:** Writing - review & editing, Supervision.

Declaration of competing interest

The authors declare that they have no known competing financial interests or personal relationships that could have appeared to influence the work reported in this paper.

Acknowledgments

This work is part of the Energy Intranets (NEAT: ESI-BiDa 647.003.002) project, which is funded by the Dutch Research Council NWO, Netherlands in the framework of the Energy Systems Integration & Big Data programme.

References

- [1] Amponsah, N.Y., Troldborg, M., Kington, B., Aalders, I., Hough, R.L., 2014. Greenhouse gas emissions from renewable energy sources: A review of lifecycle considerations. *Renewable and Sustainable Energy Reviews* 39, 461–475. URL: <https://www.sciencedirect.com/science/article/pii/S1364032114005395>, doi:10.1016/j.rser.2014.07.087.
- [2] Ayivor, P., Torres, J., 2018. Modelling of Large Size Electrolyzer for Electrical Grid Stability Studies in Real Time Digital Simulation. *International Hybrid Power Systems Workshop*.
- [3] Clegg, S., Mancarella, P., 2015. Integrated Modeling and Assessment of the Operational Impact of Power-to-Gas (P2G) on Electrical and Gas Transmission Networks. *IEEE Transactions on Sustainable Energy* 6, 1234–1244. URL: https://ieeexplore.ieee.org/abstract/document/7109157?casa_token=fhq9WAHDQw4AAAAA:v1EoS4ToVoC6nbTEAhz_D0pyzDZj-e0tGLbVpfSm0mGzgwDVeK2PZu15RIQeRjRvWZ92TRx9w, doi:10.1109/TSTE.2015.2424885. conference Name: IEEE Transactions on Sustainable Energy.
- [4] Demmel, J.W., Gilbert, J.R., Li, X.S., 1999. SuperLU users' guide. Technical Report LBNL-44289, 751785. Lawrence Berkeley National Laboratory. URL: <http://www.osti.gov/servlets/purl/751785-85h6H0/webviewable/>, doi:10.2172/751785.
- [5] Jiang, Y., Ren, Z., Yang, X., Li, Q., Xu, Y., 2022. A steady-state energy flow analysis method for integrated natural gas and power systems based on topology decoupling. *Applied Energy* 306, 118007. URL: <https://www.sciencedirect.com/science/article/pii/S0306261921013088>, doi:10.1016/j.apenergy.2021.118007.
- [6] Kabeyi, M.J.B., Olanrewaju, O.A., 2022. Sustainable Energy Transition for Renewable and Low Carbon Grid Electricity Generation and Supply. *Frontiers in Energy Research* 9. URL: <https://www.frontiersin.org/journals/energy-research/articles/10.3389/fenrg.2021.743114/full>, doi:10.3389/fenrg.2021.743114. publisher: Frontiers.
- [7] Kazi, S.R., Sundar, K., Srinivasan, S., Zlotnik, A., 2022. Modeling and Optimization of Steady Flow of Natural Gas and Hydrogen Mixtures in Pipeline Networks. URL: <http://arxiv.org/abs/2212.00961>. arXiv:2212.00961 [math].
- [8] Kiaee, M., Cruden, A., Infield, D., Chladek, P., 2014. Utilisation of alkaline electrolysers to improve power system frequency stability with a high penetration of wind power. *IET Renewable Power Generation* 8, 529–536. URL: <https://onlinelibrary.wiley.com/doi/abs/10.1049/iet-rpg.2012.0190>, doi:10.1049/iet-rpg.2012.0190. _eprint: <https://onlinelibrary.wiley.com/doi/pdf/10.1049/iet-rpg.2012.0190>.
- [9] Kweku, D.W., Bismark, O., Maxwell, A., Desmond, K.A., Danso, K.B., Oti-Mensah, E.A., Quachie, A.T., Adormaa, B.B., 2018. Greenhouse Effect: Greenhouse Gases and Their Impact on Global Warming. *Journal of Scientific Research and Reports* 17, 1–9. URL: <https://doi.org/10.9734/JSRR/2017/39630>, doi:10.9734/JSRR/2017/39630. num Pages: 9 Number: 6.
- [10] Lashof, D.A., Ahuja, D.R., 1990. Relative contributions of greenhouse gas emissions to global warming. *Nature* 344, 529–531. URL: <https://www.nature.com/articles/344529a0>, doi:10.1038/344529a0. publisher: Nature Publishing Group.
- [11] Markensteijn, A., Romate, J., Vuik, C., 2020. A graph-based model framework for steady-state load flow problems of general multi-carrier energy systems. *Applied Energy* 280, 115286. URL: <https://linkinghub.elsevier.com/retrieve/pii/S0306261920307984>, doi:10.1016/j.apenergy.2020.115286.
- [12] Markensteijn, A.S., Vuik, K., 2020. Convergence of Newton's Method for Steady-State Load Flow Problems in Multi-Carrier Energy Systems, in: 2020 IEEE PES Innovative Smart Grid Technologies Europe (ISGT-Europe), pp. 1084–1088. URL: <https://ieeexplore.ieee.org/abstract/document/9248959>, doi:10.1109/ISGT-Europe47291.2020.9248959.
- [13] Markensteijn, A.S., Vuik, K., Romate, J.E., 2019. On the Solvability of Steady-State Load Flow Problems for Multi-Carrier Energy Systems, in: 2019 IEEE Milan PowerTech, pp. 1–6. URL: <https://ieeexplore.ieee.org/abstract/document/8810916>, doi:10.1109/PTC.2019.8810916.
- [14] OSIADACZ, A.J., PIENKOSZ, K., 1988. Methods of steady-state simulation for gas networks. *International Journal of Systems Science* 19, 1311–1321. URL: <https://www.tandfonline.com/doi/abs/10.1080/00207728808547163>, doi:10.1080/00207728808547163. publisher: Taylor & Francis _eprint: <https://www.tandfonline.com/doi/pdf/10.1080/00207728808547163>.
- [15] Samani, A.E., D'Amicis, A., De Koning, J.D., Bozalakov, D., Silva, P., Vandevelde, L., 2020. Grid balancing with a large-scale electrolyser providing primary reserve. *IET Renewable Power Generation* 14, 3070–3078. URL: <https://onlinelibrary.wiley.com/doi/abs/10.1049/iet-rpg.2020.0453>, doi:10.1049/iet-rpg.2020.0453. _eprint: <https://onlinelibrary.wiley.com/doi/pdf/10.1049/iet-rpg.2020.0453>.
- [16] Savola, T., Keppo, I., 2005. Off-design simulation and mathematical modeling of small-scale CHP plants at part loads. *Applied Thermal Engineering* 25, 1219–1232. URL: <https://www.sciencedirect.com/science/article/pii/S1359431104002467>, doi:10.1016/j.applthermaleng.2004.08.009.
- [17] Schavemaker, P., Sluis, L.v.d., 2017. *Electrical Power System Essentials*. John Wiley & Sons. Google-Books-ID: Kz_CDgAAQBAJ.
- [18] Tuinema, B.W., Adabi, E., Ayivor, P.K., García Suárez, V., Liu, L., Perilla, A., Ahmad, Z., Rueda Torres, J.L., van der Meijden, M.A.,

- Palensky, P., 2020. Modelling of large-sized electrolysers for real-time simulation and study of the possibility of frequency support by electrolysers. *IET Generation, Transmission & Distribution* 14, 1985–1992. URL: <https://onlinelibrary.wiley.com/doi/abs/10.1049/iet-gtd.2019.1364>, doi:10.1049/iet-gtd.2019.1364. [_eprint: https://onlinelibrary.wiley.com/doi/pdf/10.1049/iet-gtd.2019.1364](https://onlinelibrary.wiley.com/doi/pdf/10.1049/iet-gtd.2019.1364).
- [19] Werner, S., 2013. *District Heating and Cooling*. Elsevier. URL: <https://www.diva-portal.org/smash/record.jsf?pid=diva2%3A676931&dswid=-3613>.
- [20] Zhao, P., Gou, F., Xu, W., Shi, H., Wang, J., 2023. Multi-objective optimization of a hybrid system based on combined heat and compressed air energy storage and electrical boiler for wind power penetration and heat-power decoupling purposes. *Journal of Energy Storage* 58, 106353. URL: <https://www.sciencedirect.com/science/article/pii/S2352152X22023428>, doi:10.1016/j.est.2022.106353.